First evidences of freezing tolerance in a resurrection plant: insights into molecular mobility and zeaxanthin synthesis in the dark

Authors

Beatriz Fernández-Marín[1*], Gilvert Neuner[2], Edith Kuprian[2], Jose Manuel Laza[3], Jose Ignacio García-Plazaola JI[1], Amy Verhoeven[1,4]

Affiliations

[1] Department of Plant Biology and Ecology, University of the Basque Country (UPV/EHU), Bilbao, Spain

[2] Institute of Botany, University of Innsbruck, Innsbruck, Austria

[3] Department of Physical Chemistry, University of the Basque Country (UPV/EHU), Bilbao, Spain

[4] University of St. Thomas, Biology Dept. (OWS352), University of St. Thomas, 2115 Summit Ave, St. Paul, MN 55105 USA

***Corresponding author:** beatriz.fernandezm@ehu.eus

Abstract

The photoprotective mechanisms of desiccation tolerance and freezing tolerance strategies and their relation to molecular mobility (cell vitrification) were assessed in a single model: the exceptional subalpine and resurrection plant *Ramonda myconi.* Dehydrating leaves showed a drop in F_v/F_m accompanied by synthesis of zeaxanthin (Z), even in the dark, which was limited by cell vitrification after complete desiccation. The recovery of F_v/F_m after a severe drying treatment (7 d at 50% RH) confirmed the tolerance of *R. myconi* leaves to desiccation. In winter, *R. myconi* plants showed a highly dynamic component of photoinhibition. Interestingly, the enzymatic violaxanthin de-epoxidase (VDE) activity occurred at –7 ºC, below the freezing temperature range of the leaves (2 ± 2 ºC) and even in the dark. This suggests that, in nature, the enzyme can still be active in frozen leaves, as long as they are above the glass transition temperature. Drop in F_v/F_m and increase in Z were reversible upon rehydration and thawing respectively, and were not perfectly matched, suggesting that both Z-independent and Z-dependent forms of sustained dissipation are occurring. Overall, our data reinforce the light-independent activity of the VDE enzyme under stress and suggest that Z-accumulation could occur in darkness in a scenario when temperatures drop dramatically in the night under natural conditions.

Abbreviations

A, antheraxanthin; Chl, chlorophyll; DMTA, dynamic mechanical thermal analysis; DSC, differential scanning calorimetry; DW, dry weight; F_v/F_m, maximal photochemical efficiency of PSII; FW, fresh weight; IDTA, infrared differential thermal

analysis; NPQ, non-photochemical quenching of chlorophyll fluorescence; RWC, relative water content; V, violaxanthin; Z, zeaxanthin.

Key words

Glassy state, low temperature, NPQ, photoprotection, *Ramonda myconi*

Introduction

Desiccation stress and freezing stress share many physiological consequences in photosynthetic tissues that result in severe mechanical and oxidative pressure in the cell (Verhoeven et al. 2017). The risk of exacerbated oxidative pressure occurs as a consequence of limitation to photosynthetic activity specifically, and to metabolism in general, due to dramatically slowed molecular mobility (cell vitrification) (Verhoeven et al. 2017). Under these circumstances, upregulation of photoprotective mechanisms, able either to dissipate excess absorbed light energy as heat or to protect cellular integrity from damaging oxidative reactions, becomes essential for the survival of the photosynthetic tissue (Öquist and Huner 2003; Adams et al. 2004; Chaves et al. 2009; Verhoeven 2014; Fernández-Marín et al. 2017). Different ecophysiological strategies have evolved in plants to survive frost. While some species developed freezing avoidance to deal with frost, i.e. deciduous species, or alternatively, species that undergo supercooling (Wisniewski et al. 2014), others are truly freezing tolerant and are able to cope with ice formation within their leaves (Neuner 2014). Similarly, many plant species have developed drought avoidance strategies to deal with severe limitation of water in the environment: i.e. succulent species, or drought tolerant species with very high water use efficiencies, while a few truly desiccation tolerant species, also called "resurrection plants", are able to cope with extreme dehydration until tissues equilibrate with the relative humidity of the environment (Fernández-Marín et al. 2016). Interestingly, in nature, most freezing tolerant species are not tolerant to desiccation; i.e. needles of the conifer *Picea obovata* are able to tolerate immersion in liquid nitrogen (Angelcheva et al. 2014), but no conifer has so far been described that survives to complete dehydration. At the same time, most resurrection plants are not able to tolerate freezing; so far freezing tolerance has not been reported in any of the vascular plants that are DT.

A key photoprotective mechanism used by plants to cope with excess light absorption is thermal energy dissipation, which is associated with the accumulation of zeaxanthin and is typically measured as non-photochemical quenching of chlorophyll fluorescence (NPQ). Zeaxanthin (Z) is a carotenoid that plays indispensable roles in the photoprotection and preservation of the integrity of chloroplasts. When bound to antenna proteins Z acts as a modulator of the efficiency of light energy conversion (Müller et al. 2001), and when free in the thylakoid Z participates as an antioxidant and membrane stabilizer (Havaux et al. 2004; Gruszecki and Strzalka 2005; Dall'Osto et al. 2010). Two different enzymes are capable of synthesizing Z: (i) β-carotene hydroxylase, which synthesises Z from β-carotene in a non-reversible reaction (Tian et al. 2003), and (ii) violaxanthin de-epoxidase (VDE), which catalyses the de-epoxidation of violaxanthin (V) to antheraxanthin (A) and then to Z (Saga et al. 2010). This two-step reaction has been traditionally considered to be light-dependent and can be reverted by a third enzyme: the zeaxanthin epoxidase (ZE), which epoxidates Z back to V, closing the so-called xanthophyll or V-cycle (Müller et al. 2001; Ruban et al. 2007; Demmig-Adams et al. 2012; Jahns and Holzwarth 2012; Dall'Osto et al. 2017). The conversion of V to Z is associated with conformational changes in the antennae and with enhanced dissipation of energy as heat (NPQ), that overall have a vital photoprotective role in the photosynthetic apparatus (Demmig-Adams 1998; Johnson et al. 2011; Leuenberger et al. 2017). This cycle modulates the efficiency of light energy conversion adjusting it dynamically to the actual demand of metabolic energy, thereby protecting the photosynthetic apparatus from photodamage. The payback of such a mechanism is that, in a fluctuating light environment, NPQ and energy demand are not always perfectly

coupled and NPQ may cause a loss in plant productivity up to 20% (Kromdijk et al. 2016).

Under conditions of sustained and severe stress, a non-reversible form of NPQ is activated. This has been referred to as sustained thermal dissipation and involves reductions in dark-acclimated F_v/F_m as well as dark-sustained retention of the xanthophyll pigments A and Z. This has been documented extensively in the case of winter stress (Verhoeven 2014), but is also regularly observed in response to desiccation (Fernández-Marín et al. 2016). In both stress scenarios Z has been shown to accumulate and it has been hypothesized that the A and Z are retained in a conformation for thermal dissipation, thus causing the observed reductions in F_v/F_m. However the exact role of Z on this type of NPQ has not been clearly established (Verhoeven et al. 2017). Whether dynamic and sustained NPQ represent different mechanisms or are two variations of the same process is something that requires further experiments.

While the interconversions of the xanthophyll cycle were thought to be dependent on light for decades, the independence of VDE activity from light and its direct activation solely by tissue dehydration, has been repeatedly reported in the last few years and in a wide range of phylogenetically diverse organisms. The operation of the xanthophyll cycle in darkness was first described upon desiccation/rehydration cycles in the resurrection fern *Ceterach officinarum* (Fernández-Marín et al. 2009) and later in a plethora of DT-species including lichens, intertidal macroalgae, bryophytes, and angiosperms (Fernández-Marín et al. 2010, 2011b, 2013). Synthesis of Z in darkness has also been reported during the rewarming of winter-acclimated leaves from *Quercus* species (Brüggemann et al. 2009) and during heat and anoxia stress in the intertidal macroalgae *Pelvetia canalicualta* (Fernández-Marín et al. 2011a).Though the biochemical mechanism still remains unknown, it seems reasonable that the low availability of liquid water inside the photosynthetic tissues (i.e. inside the thylakoid lumen of the chloroplast) may induce physiological changes (i.e. lower luminal pH) that are involved in the activation of VDE. The enzyme is active above a threshold of water content, below which the enzyme will be unable to operate (Fernández-Marín et al. 2013). Upon extreme dehydration of the tissues, cells go through a process, called vitrification, that ends in the glassy state: an amorphous metastable state that resembles a solid but has the disordered physical properties of a liquid and in which further loss of water and chemical reactions (particularly enzymatic reactions) are severely limited or impeded (Buitink and Leprince 2008). Once the glassy state is reached, the VDE will not be active (at least on a time frame of months) (Fernández-Marín et al. 2013). Vitrification can theoretically take place upon freezing of tissues as well, due to ice nucleation occurring extracellularly leading to desiccation of plant cells (Hirsh 1987). However literature is very scarce and inconsistent about the transition temperatures under frost, probably due to the technical limitations of the traditionally used differential scanning calorimetry (DSC) technique to assess frozen photosynthetic tissues such as leaves (Hirsh 1987; Strimbeck and Schaberg 2009; Strimbeck et al. 2015). Other approaches such as dynamic mechanical thermal analysis (DMTA) successfully used with seeds or with dry photosynthetic tissues may help to shed light on this aspect (Fernández-Marín et al. 2013). Considering the biophysical similarities that consequences of desiccation and of freezing have on plant leaves (i.e. removal of most of the bulk liquid water from the cell), we hypothesise that (i) Z could be synthesised during freezing even in the absence of light in a mechanism similar to that which occurs during desiccation and (ii) the enzyme will remain active before cellular content is vitrified. Furthermore, we speculate that (iii) if Z is formed upon freezing, it

will contribute to the photoprotective capacity of the tissue, and in particular to a sustained mode of NPQ, during the next morning.

All things considered, it is pertinent to assess the photoprotective mechanisms of desiccation tolerance and freezing tolerance strategies and their relation to molecular mobility (cell vitrification) in a single model plant. We have chosen for this purpose the angiosperm *Ramonda myconi* (Fam. Gesneriaceae), one of the only five resurrection species native to Europe (Rakic et al. 2015), endemic to the Pyrenees mountains and that can reach the subalpine level, growing even at elevations higher than 2000 m a.s.l. (Picó and Riba 2002). Being a slow-growing evergreen, its leaves are unavoidably exposed to long periods of temperatures well below the freezing point. Further, considering its preference for vertical limestone slopes that are usually North oriented, where winter frost is unlikely buffered by the snowpack, we hypothesise that *R. myconi* plants must have developed freezing tolerance. Overall, our goal was to assess the photoprotective mechanisms that underpin both desiccation and freezing tolerance in *R. myconi* plants with a particular focus on xanthophyll cycle operation in response to both desiccation and freezing temperatures. Specifically we attempt to (i) characterise winter photoprotection of *R. myconi* as an exceptional evergreen resurrection and subalpine plant, (ii) evaluate the vitrification of photosynthetic tissue under low temperature, and (iii) assess whether or not the synthesis of Z can be directly triggered by freezing (i.e. in darkness), as observed during desiccation in other organisms.

Materials and methods

Plant material

All freezing experiments were performed in winter during two consecutive years, 2016 and 2017 (Feb 2016, Dec 2016, Mar 2017), with outdoor plants from the Botanical Garden of the University of Innsbruck, in Innsbruck, Austria (47°16′N, 11°23′O, 600 m a.s.l.). The studied plants were first planted at the Botanical Garden in 1989 and have their origin in native populations of the Pyrenees. Since then they have been growing outdoors on a limestone substrate with North-West orientation, and receive no artificial watering from September to May. Watering only occurs during hot summers and is on a weekly basis. Desiccation experiments were done with leaf material collected in late spring (May 2016) from a natural population of *R. myconi* growing in San Juan de la Peña, Aragón, Spain, in the Pyrenees (42°30′N, 0°40′W, 1150 m a.s.l). Plants were inhabiting a vertical limestone wall, facing North-West, in the understorey of a deciduous mixed forest. Only mature healthy leaves were used for experiments (second level of the rosette from the ground).

Experimental design

Experiment 1: Desiccation in the dark. Leaf discs of 12.5 mm diameter were detached from hydrated spring leaves and subjected to a desiccation-rehydration cycle in darkness. Controlled desiccation was conducted by equilibrium of samples with a saturated solution of $MgCl_2$ at a relative humidity (RH) of 50%. Maximal photochemical efficiency of PSII (F_v/F_m) and relative water content (RWC) were monitored at time points: 0, 5, 24, 72, and 168 h during desiccation, and at 15 min, 2 h,

4 h and 24 h during rehydration. Relative water content was estimated as: [(FW-DW)/(TW-DW)] * 100, where FW is actual weight, TW is turgor weight and DW is weight after drying the leaf discs in the oven at 80 ˚C for 48 h. The de-epoxidation state of the xanthophyll cycle (abbreviated as AZ/VAZ) was assessed at 0, 24 and 168 h during desiccation. Additionally, molecular mobility of leaf tissues was assessed on a separate set of samples after equilibration at 50% RH for 48 h, by dynamic mechanical thermal analysis (details below).

Experiment 2: Controlled-freezing in the dark. Freezing experiments were performed inside of a temperature-controlled commercial chest freezer (GT 2102, Liebherr, Lienz, Austria). The temperature runs inside the freezing compartment can be pre-programmed with a special software (written in Lab-View 2012 by O. Buchner). Temperature is controlled against the permanently cooling chest freezer by the use of heaters (Possitive Temperature Coefficient heater, Nimbus B200, DBK Austria, Krems, Austria) at AND accuracy of ± 0.2 ˚K. The freezing runs were programmed to start at +4 ˚C, which was initially kept for 1 h. The temperature was then lowered at 2 ˚K h^{-1}, until a minimum of –7 ˚C was reached. This temperature profile was close to the maximum cooling rates that can naturally occur below 0 ˚C in alpine regions (Neuner et al. 2013). Naturally winter-acclimated leaves of *R. myconi* plants were collected in the field the afternoon before the experiment, when the air temperature was around +4 ˚C. The petiole was immediately immersed in water and each leaf incubated overnight in darkness and at +4 ˚C for 16 h before conducting the freezing experiments the next morning. Leaf temperature was monitored with six thermocouples during the freezing. In the first experiment, actual fluorescence emission (F_0) and infrared images of whole winter acclimated leaves (Feb 2016) were monitored during freezing on four individual leaves (details below) and F_v/F_m measurements were recorded at the beginning and the end of the freezing. In order to assess pigment changes during freezing treatments, experiments were repeated in December of 2016. In this experiment F_v/F_m was measured, and samples were collected for pigment analysis before and after a freezing treatment (n = 4). In a third replicate of the experiment (Mar 2017), in order to assess whether a longer exposure to freezing conditions would impact the xanthophyll pigment composition, a set of 6 leaves from separate individuals was subjected to the same freezing conditions, but incubated for 16 h at –7 ˚C in the dark.

Experiment 3. Winter photoinhibition and recovery kinetics in R. myconi. Natural predawn F_v/F_m values were recorded directly in the garden (before sunrise) from intact plants on multiple winter mornings to establish a correlation with air temperature. Additionally, a recovery experiment was performed to determine (i) whether there is a fast and slow component in the recovery of photochemical activity of winter-acclimated *R. myconi* leaves and (ii) whether a correlation exists between F_v/F_m and AZ/VAZ during the recovery process. The recovery experiment was performed on the 15th of December 2016. Initial F_v/F_m values were measured on intact leaves outdoors. The same leaves were then collected in the early morning when air T was –2 ˚C, and immediately transferred (with the petiole immersed in water) to the lab for an initial incubation of 1h at 4 ˚C in darkness. Leaves were then transferred to +20 ˚C in darkness. The F_v/F_m values and the de-epoxidation index of xanthophyll cycle were recorded at 0, 1, 5 and 24 h during rewarming.

Determination of molecular mobility

Mechanical analyses of *R. myconi* leaves either desiccated (equilibrated at 50% RH) or fully hydrated were conducted. This measurement provided information about the extent of molecular mobility (and thus the potentiality of enzymatic activity) at a wide range of temperature including that when *R. myconi* leaves are frozen. Mechanical analyses were conducted using a DMA/SDTA861e mechanical thermal analyser (Mettler Toledo, Switzerland) in the shear mode. The method used is similar as previously described in (Fernández-Marín et al. 2013) with small modifications: tests were carried out in the dynamic mode from -50 to +150 ˚C at a heating rate of 2 ˚C min^{-1}. Each sample was scanned twice. Shear storage modulus (G´), shear loss modulus (G") and the loss tangent (tanδ = G"/G´) were calculated using the Mettler Toledo START^e software during dynamic mechanical thermal analysis (DMTA) scans.

Assessment of ice nucleation and propagation through thermal imaging

Ice nucleation and propagation within *R. myconi* leaves were monitored with a digital infrared camera (T650SC, FLIR Systems, Dandervd, Sweden) of 0.2 mK thermal resolution. The camera was equipped with a close-up lens (magnifying factor: 1.5X, working distance: 46 mm) to achieve a spatial resolution of 25 µm. Images were recorded at a rate of 10 frames per second, and then processed by Infrared Differential Thermal Analysis (IDTA) (Hacker and Neuner 2007) with the FLIR software ResearcherIR Max (version 4.20.2.74, FLIR Systems, Dandervd, Sweden). Briefly, we subtracted as reference image the IR frame just before the occurrence of ice nucleation. The result is a sequence of images showing only the changes in temperatures, i.e. the pattern of latent heat released during freezing of water in plants. Analysed leaves of *R. myconi* were free of surface moisture to allow identification of sites of intrinsic nucleators (Pearce 2001). After detachment, the entire sample, including the cut surface, was subjected to freezing temperatures. To have the entire sample in focus, leaves were flattened against a clear metallic plate and fixed by double-sided adhesive tape. In order to prevent artificial supercooling of the leaf, ice nucleation in the petiole was triggered around –3.3 °C by application of a droplet of INA (Ice Nucleation Active) bacteria suspension (*Pseudomonas syringae* van Hall 1902; Leibniz Institut DSMZ-Deutsche Sammlung von Mikroorganismen und Zellkulturen GmbH, Braunschweig, Germany) at the cut end of the petiole.

Determination of freezing temperature in R.myconi leaves

To establish the freezing temperature of *R. myconi*, 12-14 mg size leaf samples (main veins of the blade were avoided) were analysed by Differential Scanning Calorimetry (DSC 822e from Mettler Toledo, Switzerland). Samples were sealed in aluminium pans and were characterized under constant nitrogen flow (20 mL min^{-1}). First, samples were equilibrated at +4 ˚C, and then cooled at a rate of 0.035 ˚C·min^{-1} (which is equivalent to the 2 ˚K·h^{-1} cooling rate used in the IDTA analysis, see above) from +4˚ to –14 ˚C. After DSC scans, samples were dried for 24 h in an oven at 80 ˚C and dry weight recorded, for the estimation of the water content (WC). Before the measurements, the DSC equipment was calibrated with zinc, indium and pure water as standards. All weights were recorded using a Mettler Toledo 0.1 mg precision balance. DSC experiments were performed at least three times.

Photosynthetic pigment analysis

Approximately 15 mg of fresh leaf material (equivalent to around 5 mg of Dry Mass DM) were used per replicate, and 4 to 6 replicates per treatment and/or time point for photosynthetic pigment analysis. Samples were immediately frozen in liquid nitrogen after treatment and freeze-dried before analysis. The method described in (García-Plazaola and Becerril 2001) was followed with small modifications. Briefly, samples were double extracted in 0.250 mL of cold (+4 ˚C) Acetone:Water (95:5 v:v) first, and in 250 mL of pure acetone second. All acetone solutions were buffered with $CaCO_3$. Both supernatants were filtered through a 0.2 µm PTFE filter (Teknokroma, Barcelona, Spain) before being analysed by HPLC. The relative de-epoxidation state of the xanthophyll cycle pigments was estimated by the ratio (A+Z)/(V+A+Z), abbreviated AZ/VAZ.

Chlorophyll fluorescence measurements

Chlorophyll *a* fluorescence was measured with a Mini-PAM Chl fluorometer system (Heinz Walz, Effeltrich, Germany) for all freezing and low temperature experiments and with a PAM2500 (Walz, Effeltrich, Germany) for the desiccation experiment. Samples were incubated in darkness, for at least 30 min, before F_0 and F_m measurements. These were then used to estimate maximal photochemical efficiency of PSII (F_v/F_m). In Experiment 2, the fluorometer probe was fixed with a 60º angle at approximately 5 mm from the leaf (without direct contact to avoid alterations in the ice nucleation) and F_0 was monitored along the freezing cycle.

Statistical analyses

One-way ANOVA, with Duncan test as *post hoc,* was applied to test for significant differences among treatments whenever raw or log-transformed data showed homoscedascity. Wilcoxon H-test followed by Mann-Whitney U-test was used for data showing heteroscidasticity. In controlled-freezing experiment paired t-test was used to assessed for significant differences in F_v/F_m and AZ/VAZ before and after freezing of the leaves. All statistical analyses were run with SPSS v24.0 at a significance level of $\alpha = 0.05$.

Results

Desiccation of Ramonda myconi leaves in the dark

Ramonda myconi plants survive complete desiccation as shown in Fig. 1. During a desiccation event, leaves shrink and amazingly reduce their area by means of 60-70 % (data not shown) (Fig. 1C). Chlorophyll content is maintained, and initial leaf area, turgor and healthy appearance are completely re-gained after rehydration (Fig. 1D).

A controlled dehydration of leaf discs performed at 50% RH in the dark, induced a significant decrease in the F_v/F_m from initial values of 0.75 ± 0.01 (average ± SE) to final values of 0.49 ± 0.02 after 168 h of dehydration (Fig. 2A). While the majority of water loss occurred in the first 6 h of desiccation, the main decrease in F_v/F_m took place later, after minimum water content had been reached (Fig 2A, B). One day after the onset of desiccation (t=24 h), RWC was already below 5%, reaching a minimum of 3.8 % ± 0.0 at 168 h of exposure to 50 % RH atmosphere (Fig. 2B). This final RWC was

equivalent to an absolute water content of 0.12 ± 0.01 g H_2O g^{-1} DW. After rehydrating (still in the dark), the F_v/F_m increased towards initial values, up to 0.62 ± 0.01, although complete recovery was not reached by the end of the experiment, 24 h after the onset of the rehydration. Desiccation, even when it took place in complete darkness, induced the de-epoxidation of xanthophyll cycle pigments, i.e.: a significant amount of A+Z was accumulated within the first 24 h (Fig. 2C), resulting in a three-fold increase in AZ/VAZ after 24 h of desiccation. No additional de-epoxidation occurred during the remaining several days in the desiccated state (Fig. 2C, 168 h). The total pool of xanthophyll cycle pigments, expressed as a function of total chlorophyll, did not change significantly (Fig. 2D). Observed changes in the AZ/VAZ, matched the significant increase in Z/Chl (Fig. 2E) upon drying.

Molecular mobility in dry vs frozen leaves

Dynamic mechanical thermal analysis (DMTA) allows for an assessment of the relative molecular ability of a sample as a function of temperature. The alpha relaxation, which corresponds to the transition from glass to gel phases, can be identified as a peak in the Tan δ and as a steep decline in the storage modulus (G'). DMTA was performed on both hydrated and desiccated *R. myconi* leaf tissue in order to assess changes in relative molecular mobility as a function of temperature in both the hydrated and desiccated state. Analysis of fully desiccated *R. myconi* leaves (equilibrated to 50% RH atmosphere) revealed extremely low molecular mobility at ambient temperature ≈ +20 ˚C (Fig. 3A, B). Alpha relaxation appeared in the range of +20 to +40 ˚C. Thus, at ambient temperature (≈+20 ˚C), or below, *R. myconi* dry leaves were in the glassy state and enzymatic reactions are very unlikely (virtually impossible in a human time-scale) (Fig. 3A, B). In agreement with this, AZ/VAZ ratio remained unaltered after drying, i.e.: no significant difference was found between the timepoints 24 and 168 h after desiccation (see Fig. 2C). When hydrated leaves were subjected to the same DMTA analysis, the thermogram showed an expected shift of the α-relaxation towards lower temperatures (Fig. 3C, D). Noticeably, the glassy state was reached at temperatures below –15 ˚C, so although slowed down, enzymatic reactions could be expected at temperatures above –15 ˚C in frozen *R. myconi* leaves.

Regulation of photochemical efficiency in winter-acclimated leaves of Ramonda myconi

Winter acclimated plants of *Ramonda myconi* (Fig. 1B) showed a highly dynamic component of photoinhibition (by means of reduction in F_v/F_m) (Fig. 4). Measured at natural predawn, F_v/F_m decreased moderately (≤ 0.5) at air temperatures around 0 ˚C, while severe photoinhibition (F_v/F_m < 0.1) occurred in frozen leaves, whenever air temperature was ≤ 5 ˚C (Fig. 4, dates: 9th, 16th and 18th Dec, and some of the leaves on the 15th Dec). The dynamic nature of the photoinhibition was evidenced by the direct relationship between the extent of photoinhibition and the air temperature, but not between the extent of photoinhibition and the date. In other words decreasing F_v/F_m values did not follow correlative dates (as it could happen during winter acclimation in other plants), but followed a decreasing trend towards lower air temperatures (Fig. 4).

The dynamic component of this observed winter photoinhibition is also observed in winter recovery experiments (Fig. 5). Leaves collected in the field at –2 ˚C and incubated at +20 ˚C in darkness, recovered the main proportion of their F_v/F_m within the first hour (Fig. 4A). The recovery of F_v/F_m was accompanied by re-epoxidation of

AZ/VAZ (Fig. 5B), as also evidenced by the decrease in the Z content (Fig. 5C), and without significant change on the size of the total VAZ pool (Fig. 5D). This was evident in the second phase of the photochemical recovery (i.e. after the first hour). Nevertheless, and noticeably, the initial recovery in F_v/F_m from 0.12 ± 0.04 (at time 0) to 0.45 ± 0.06 (at time 1 h) took place without significant change in the AZ/VAZ or in the Z/Chl ratios (Fig. 5A-C).

Ice nucleation and propagation pattern, photochemical efficiency and xanthophyll cycle activation during controlled freezing of R. myconi *leaves in the dark*

Controlled freezing experiments involved placing winter acclimated *R. myconi* leaves, that had incubated at +4 ˚C in darkness overnight, into a freezing chamber where temperatures were lowered at a rate of –2 ˚K h^{-1} in darkness. The process of freezing was monitored with an infrared camera (Fig. 6), and F_0 values were recorded in parallel with a fluorometer probe (Fig. 6A, 7A).

During the process of freezing two different phases were distinguishable (Fig. 6). In the first phase, ice nucleation started at the petiole and propagated through the main vein from the bottom to the tip of the leaf (Fig. 6B). From there, ice propagated throughout the edges of the leaf from the tip to the base following its venation pattern: from the leaf margin, the ice front moved back towards the mid-vein (Fig. 6B, C). A second phase of freezing started approximately 6 min later (Fig. 6D). During the second phase of the freezing, the mesophyll started to freeze at different isolated nucleation points, randomly throughout the blade (Fig. 6D, E). The whole freezing process lasted 10-20 min and took place at a leaf temperature range between –1 and –4 ˚C. This was in agreement with the freezing temperature of *R. myconi* leaves revealed from the DSC (Fig. 6F). A clear exothermic peak was observed around a sample temperature of –2 ˚C when running scans at a comparable freezing rate of 0.035 ˚C min^{-1}.

Initial readings of F_v/F_m and AZ/VAZ were assessed prior to freezing the leaves and showed relatively high values for photochemical efficiency and relatively low amounts of A+Z present (Fig. 7B, C). The chlorophyll fluorescence parameter F_0 was monitored throughout the cooling process (Fig. 7A). A sharp decline in F_0 was observed starting around –3 ˚C, which is the time point coincident with ice formation in the leaf area just below the fluorescence probe (equivalent to figure 6E), until reaching minimum levels at a temperature of around –6 ˚C (Fig. 7A). Additionally, F_v/F_m values were reduced significantly during the freezing treatment in darkness, although the extent of reduction was quite variable (Fig. 7B). Values for F_v/F_m were 0.66 ± 0.07 (average ± SE) before freezing, and decreased to quenched values of 0.41 ± 0.25 after the freezing treatment (Fig. 7B).

Pigments were collected before and after the freezing treatment, however analysis showed no change in xanthophyll cycle pigments as a result of freezing in darkness (data not shown). Nevertheless, since DMTA analysis revealed a high probability for enzymatic reactions to take place at –7 ˚C in *R. myconi* leaves, although at lowered rate (Fig. 3C, D), a longer incubation was performed in darkness at –7 ˚C on a second set of leaves. In this experiment a more natural night was simulated by incubating the leaves at –7 ˚C for 16 h in darkness. In this case AZ/VAZ increased two fold (Fig. 7C), which corresponded to a significant increase in the content of Z (Fig. 7D). This result indicates that freezing can directly induce Z synthesis in the absence of light.

Discussion

Desiccation tolerance in R. myconi

While most resurrection plants described so far have their native habitats in tropical areas of the South Hemisphere (Porembski and Barthlott 2000), *Ramonda myconi* is one of the few resurrection angiosperms in Europe (Rakić et al. 2014). There are five European resurrection plant species, which represent preglacial endemo-relict examples of the tropical-subtropical family Gesneriaceae. *R. myconi* is the only one growing in the Iberian Peninsula (it is endemic to the Pyrenees) while the other four: *R. serbica*, *R. nathaliae*, *Haberlea rhodopensis* and *Jankaea heldreichii* grow in the Balkan Peninsula (Rakić et al. 2014). Surprisingly, most of the research conducted with *R. myconi* has dealt with molecular aspects related to its polyploidy, phylogeny, and biogeography, or focused in the development of protocols for its *in vitro* culturing and transformation (Tóth et al. 2004, 2006; Dubreuil et al. 2008; Siljak-Yakovlev et al. 2008). Only a couple of works aimed at unravelling its ecology (Picó and Riba 2002; Riba et al. 2002), and very scarce literature regards its ecophysiological performance (Schwab et al. 1989). This, contrasts with the extensive ecophysiological assessment of its Balkan relatives *R. serbica*, *R. nathaliae* and *H. rhodopensis* (Müller et al. 1997; Georgieva et al. 2007; Degl'Innocenti et al. 2008; Dubreuil et al. 2008; Rakic et al. 2015; Rapparini et al. 2015), with which *R. myconi* shares habitat preferences: i.e. limestone crevices. Although *R. myconi* has been assumed to be a resurrection plant, because all other species of the genus are tolerant to desiccation (reviewed in (Rakić et al. 2014)), we provide in this work ecophysiological evidence of its ability to resume normal metabolic activity after drying (Fig. 1C, D, Fig. 2).

The observed decrease in F_v/F_m upon desiccation of *R. myconi* leaves was much more moderate than what has been reported for bryophytes or lichens, but is consistent with values reported for other resurrection plants; i.e. F_v/F_m values > 0.3 were measured in dry leaves of *R. serbica* (Gashi et al. 2013), *R. nathaliae* (Fernández-Marín et al. 2011b), *H. rhodopensis* (Rapparini et al. 2015) or *Craterostigma pumilum* (Charuvi et al. 2015); and F_v/F_m values > 0.4 were obtained in *R. nathaliae* (Gashi et al. 2013) or in dry fronds of the DT-fern *Hymenoglossum cruentum* (Flores-Bavestrello et al. 2016). The drop in F_v/F_m shown by *R. myconi* was accompanied by synthesis of Z, even in the dark (Fig. 2), as previously shown for other tracheophytes tolerant to desiccation, including angiosperms (Fernández-Marín et al. 2009, 2011b). This finding reinforces the light-independence of the enzyme VDE under desiccation conditions, and the relevance of Z for the preservation of thylakoid integrity and functionality upon drying (Kranner et al. 2002; Beckett et al. 2012; Fernández-Marín et al. 2013). The decline in F_v/F_m was delayed in comparison to the loss of water content indicating a non-direct relationship between RWC and regulation of photochemical efficiency. According to the DMTA analyses (Fig. 3A, B) leaves of *R. myconi* totally equilibrated to 50% RH (i.e. dry) would be in the glassy state at temperatures <20 ˚C and thus, enzymatic reactions would very unlikely within the cell. This matches with the unaltered AZ/VAZ ratio found between the time points 24 and 168 h after desiccation (Fig. 2C). The recovery of F_v/F_m after a severe drying treatment (7 d at 50% RH, which is equivalent to an atmospheric ψ_w = –93.6 MPa) confirms the tolerance of *R. myconi* leaves to desiccation (Fig. 2A).

First evidence of freezing tolerance in a resurrection plant

Although freezing tolerance is reasonably probable in some resurrection plants from temperate regions, there is very scarce literature about their physiology under low temperature conditions. Benina et al. (2013) have described metabolic changes in *Haberlea rhodopensis* subjected to +4 ˚C for 3 d in a chamber, but no literature is available about the performance of resurrection plants in subzero temperatures, except for one attempt to evaluate resistance to low temperature of *R. myconi* leaves, that consisted in the description of their survival to immersion in liquid nitrogen, when desiccated (Kappen 1966). Thus, to the best of our knowledge, we provide here the first evidence for the tolerance of a resurrection plant's (i.e. *R. myconi*) leaves to intratissular ice formation, and thus its tolerance to freezing, as extracellular ice formation was tolerated without any damage to the leaves. The ice nucleation temperature of the leaves, estimated *ex situ*, was slightly higher (≈ –2 ± 2 ˚C; Fig. 6F, Fig. 7B) but consistent with observations in the field, when air temperature ≤ –5 ˚C resulted in dramatic declines in F_v/F_m (Fig. 4).

Rapid vs slow components to recovery from winter stress in R. myconi

Studies on overwintering evergreens have relied on measurements of recovery of F_v/F_m upon warming winter-acclimated photosynthetic tissue as a method for learning something about the mechanisms of reduced F_v/F_m that occur at least in part due to sustained forms of thermal dissipation (Verhoeven, 2014). Such studies have demonstrated that the kinetics of recovery consists of two phases that differ in relaxation rate; an initial phase relaxes very rapidly (within minutes to hours) while a second phase relaxes more slowly (hours to days) (Ottander and Oquist 1991; Verhoeven et al. 1996). The extent of each component varies widely depending upon species, light environment, temperature and the extent of the winter season (Verhoeven et al. 1998; Verhoeven 2013; Míguez et al. 2017). The slower component of sustained dissipation has been widely reported in overwintering conifers as well as broad-leaved evergreens and is the dominant form of sustained dissipation observed in severe midwinter conditions (Ottander and Oquist 1991; Verhoeven et al. 1996; Míguez et al. 2015). The rapid component of sustained dissipation has been less widely reported but, importantly, is characterized by only occurring in conditions when temperatures drop below 0 ˚C (Míguez et al. 2015). This form of sustained dissipation seems to be more common earlier in the winter season, and is a larger component in plants acclimated to shadier environments (Verhoeven 2013). Previous studies have suggested that both the rapid and slowly reversible components of sustained thermal dissipation involve sustained engagement of xanthophyll pigments A+Z (Demmig-Adams and Adams 2006).

The recovery of winter stressed *R. myconi* leaves demonstrated a pronounced rapid component to recovery, with F_v/F_m values rising from 0.12 to 0.45 within the first hour of warming, while a slower component occurred over the next several hours with F_v/F_m rising to 0.63 after 5 hours of warming (Fig. 5A). Interestingly, the values for AZ/VAZ which were high at time zero remained high after 1 hour of warming and didn't decline until the five hour time-point, suggesting that F_v/F_m and AZ/VAZ are not tightly coupled during the initial rapid component of recovery. The observation that *R. myconi* had a pronounced rapidly-reversible component to its sustained dissipation is consistent with the leaves being collected in conditions when temperatures were below 0 ˚C and the fact the plant is adapted to low light conditions as it grows most commonly on North-facing slopes.

The observed variation in predawn F_v/F_m as a function of air temperature also supports the finding that *R. myconi* leaves have a substantial rapid component to sustained thermal dissipation (Fig. 4). F_v/F_m values were reduced in a temperature dependent manner, with larger reductions occurring on the coldest days, while on dates when temperatures were above zero values clustered around 0.5. This demonstrates dynamic regulation of photochemical efficiency tied to leaf temperature, presumably allowing for maximal thermal dissipation on subzero days when low temperatures would preclude photosynthetic carbon gain. These data are consistent with previous studies showing a close relationship between predawn F_v/F_m and air temperature (Lundmark et al. 1998).

Light-independent reductions in F_v/F_m and de-epoxidation of V to Z can be induced by low temperatures

One of the goals of this study was to explore the mechanism of sustained forms of thermal dissipation in a comparative context by exploring whether reductions in F_v/F_m and Z formation can occur in the absence of light as a function of both desiccation and low temperatures. Previous studies have reported dark formation of Z in response to desiccation in a variety of species (see above). Indeed, light-independent de-epoxidation of V to Z, has repeatedly been demonstrated under different stress conditions throughout the last decade (Brüggemann et al. 2009; Fernández-Marín et al. 2009, 2011a; Buchner et al. 2015). The operation of the xanthophyll cycle in darkness was first described upon desiccation/rehydration cycles in the resurrection fern *Ceterach officinarum* (Fernández-Marín et al. 2009) and later in a plethora of DT-species including lichens, intertidal macroalgae, bryophytes, and angiosperms (Fernández-Marín et al. 2010, 2011b, 2013). We hypothesized that if reductions in F_v/F_m and formation of Z occurs in darkness during desiccation, due to mechanistic changes associated with the physical process of desiccation, this may also occur as a result of desiccation associated with freezing. Our results demonstrated significant reductions in F_v/F_m consistently occurred in response to freezing *R. myconi* leaves in darkness, although the extent of the reduction of F_v/F_m was highly variable (Fig. 7). An initial experiment examining A+Z content after cooling from +4 ˚C to –7 ˚C at a rate of –2 ˚C per hour showed no accumulation of A+Z, again illustrating a decoupling of the reduction in F_v/F_m and A+Z content. However, very interestingly, there was a significant increase in the de-epoxidation index of xanthophyll cycle pigments in *R. myconi* leaves after incubation at –7 ˚C for a period of 16 hours (Fig. 7). This finding reinforces the light-independent activity of the VDE enzyme under stress by providing the first evidence about the synthesis of Z can be directly induced by freezing (in the absence of light). This suggests that Z-accumulation could occur in darkness in a scenario when temperatures drop dramatically in the night under natural conditions.

Interestingly, the enzymatic VDE activity occurred below the freezing temperature range of R. *myconi* leaves (Fig. 6), which suggests that, in nature, VDE can still be active in frozen leaves, as long as they are above the glassy state (i.e. at higher temperatures than the alpha-relaxation Fig. 3). Our evidence from direct mechanical measurements of hydrated leaves through DMTA are consistent with the hypothesis that in frozen leaves of *R. myconi*, enzymatic activity is still possible above –15˚C (Fig. 3C, D).

So far, the possibility of leaf vitrification upon freezing had been suggested (Strimbeck and Schaberg 2009; Strimbeck et al. 2015) but very scarce measurements in photosynthetic tissues, i.e. leaves, had been conducted and most of them were

performed through low accuracy methodologies such as DSC (Hirsh 1987). From polymer sciences, it is long known that DMTA is a method with great sensitivity in detecting changes in internal molecular mobility (Laza et al. 1999). In the plant sciences, Ballesteros and Walters demonstrated that DMTA is a very accurate technique for directly measuring molecular mobility in dry seeds (Ballesteros and Walters 2011) and Fernández-Marín and co-workers estimated glass transitions in leaves from a desiccation tolerant bryophyte and related the vitrification to the limitation of enzymatic reactions (Fernández-Marín et al. 2013). The higher sensitivity of DMTA over DSC for the detection of glass transitions in polymers such as starch has recently been reported (Zhang et al. 2014). The successful estimation of glass transitions in frozen *R. myconi* leaves shown in this work, may serve as a baseline for future work to enhance our understanding of biochemical and physiological mechanisms of freezing tolerance in plants.

Towards understanding the mechanism(s) of sustained thermal dissipation

One of the goals of this study was to explore the mechanism(s) of sustained thermal dissipation by examining sustained dissipation in a single species that is tolerant to two forms of extreme stress that both result in induction of sustained forms of thermal dissipation. Previous studies on low temperature stress have suggested that low-temperature induced sustained dissipation may involve sustained forms of the dynamic nonphotochemical quenching (NPQ) (Verhoeven 2014). This hypothesis is based on a model put forth by Holzwarth et al. (2009) suggesting two forms of thermal dissipation that differ in mechanism, location and relaxation time. It was suggested that the rapid component to sustained dissipation may be a sustained form of the so-called "Q1" type of quenching proposed by Holwarth et al. which is suggested to require PsbS, and ΔpH across the thylakoid membrane but can be independent of Z. The slower component was suggested to be a sustained form of the "Q2" type of quenching that requires Z but is independent of ΔpH and PsbS (Holzwarth et al. 2009). Our data from *R. myconi* are consistent with this hypothesis, as *R. myconi* shows a large rapid component of sustained dissipation that seems to be independent of Z formation, while a smaller slow component to recovery correlated closely with reconversion of Z to V. Our data are suggestive that similar mechanisms may be occurring in response to desiccation, as the F_v/F_m showed both a rapid and slower component to recovery upon rehydration (Fig. 2A). Interestingly, the onset of freezing in the mesophyll of *R. myconi* was coincident with a marked drop in the F_0 (Fig. 7A) that contrasts with the response usually observed in leaves of species non-tolerant to desiccation. In the later, F_0 was found to increase, after a species-specific time lag after ice nucleation of between 10 to 26 min (Neuner and Pramsohler 2006; Hacker et al. 2008). The unexpected decrease of F_0 found in the resurrection plant *R. myconi* would be in agreement with the de-activation of PSII before PSI, that has been described in desiccation tolerant species upon severe tissue dehydration (Nabe et al. 2007; Kosugi et al. 2009; García-Plazaola et al. 2012). Future research would be needed to better understand this mechanism of basal fluorescence quenching that probably underpins photoprotection of photosynthetic apparatus under both freezing and dehydrating conditions in desiccation tolerant plants.

Despite its partial decoupling from energy dissipation, the synthesis of Z solely triggered by freezing in darkness, indicates a crucial role for this carotenoid upon freezing. The accumulation of Z may have important roles beyond energy dissipation, as previously suggested in dry bryophytes (Fernández-Marín et al. 2013). Other hypothesized roles for Z, such as the safe packing of photosynthetic protein complexes

and the preservation of thylakoid membrane integrity (Johnson et al. 2011; Jahns and Holzwarth 2012; Ilioaia et al. 2013), may be indispensable for frozen photosynthetic tissues.

The light dependence of the conversion of xanthophyll cycle pigments, and therefore the engagement of sustained thermal dissipation, is interesting from a mechanistic viewpoint, as our current understanding of the requirements for the activation of thermal dissipation relies on the establishment of a proton gradient derived from photosynthetic electron transport. In most relevant physiological scenarios plants exposed to extreme stress exist in a dynamic light environment which would result in some formation of A and Z during the times of light exposure that might then be retained in darkness to provide the observed sustained dissipation. However, studies showing that Z formation can occur in the absence of light, due directly to desiccation or desiccation associated with freezing conditions (as shown here) suggest that VDE must be activated via alternative mechanisms, possibly due to conformational changes associated with the reduced cell volume that occurs in such conditions. Further studies are needed to explore a mechanistic understanding of these observations.

Concluding remarks

Both desiccation and freezing conditions triggered (i) synthesis of Z (even in the absence of light) and (ii) reductions in the maximal efficiency of photochemistry (F_v/F_m) in the leaves of the resurrection plant *R. myconi*. These changes were reversible upon rehydration and thawing respectively, and were not perfectly matched, suggesting that both Z-independent and Z-dependent forms of sustained dissipation are occurring. In winter leaves, enzymatic reactions (i.e. de-epoxidation of V to A+Z by VDE) took place below the freezing temperature range and above the alpha-relaxation temperature, in which the cellular content had a considerably high viscosity but with molecular mobility still possible to some extent. These findings could be interpreted in agreement with the hypothesis that desiccation tolerance mechanisms of *R. myconi* provide the basis of its resistance to frost that may have allowed this (and maybe its close Balkan relatives) to remain as the relict tertiary tropical species which survived the glacial era in the European continent (Rakić et al. 2014).

Author contribution

BFM, AV and JIGP designed the work. AV conducted the desiccation experiments. BFM, AV, EK and GN conducted the freezing experiments. BFM and JML conducted DMTA and DSC analyses. JIGP and BFM drafted the manuscript. All co-authors contributed to final version of the manuscript.

Acknowledgements

We want to thank P Schönswetter, M Houlobek, M Imhiavan and PD Schlorhaufer for their valuable support regarding the study of *Ramonda myconi* plants from the Botanical Garden of the Institute of Botany (University of Innsbruck, Innsbruck, Austria). We also thank the "Instituto Aragonés de Gestión Ambiental (INAGA), Departamento de Desarrollo Rural y Sostenibilidad, Gobierno de Aragón" for permission to study natural

populations of *Ramonda myconi* in San Juan de la Peña (Aragón, Spain).

Funding

Financial support from Basque Government (UPV/EHU IT-1018-16 and UPV/EHU IT-718-13); Spanish Ministry of Economy and Competitiveness (MINECO) and the ERDF (FEDER) (CTM2014-53902-C2-2-P) to J.I. G.-P., A.V. and B. F.-M.; and "Juan de la Cierva-Incorporation" fellowship IJCI-2014-22489 to B.F-M.; and University of St. Thomas Sabbatical Assistance Grant to A.V. are acknowledged.

References

Adams WW, Zarter CR, Ebbert V, Demmig-Adams B (2004) Photoprotective strategies of overwintering evergreens. Bioscience 54:41–49. doi: 10.1641/0006-3568(2004)054[0041:PSOOE]2.0.CO;2

Angelcheva L, Mishra Y, Antti H, et al (2014) Metabolomic analysis of extreme freezing tolerance in Siberian spruce (*Picea obovata*). New Phytol 204:545–555. doi: 10.1111/nph.12950

Ballesteros D, Walters C (2011) Detailed characterization of mechanical properties and molecular mobility within dry seed glasses: Relevance to the physiology of dry biological systems. Plant J 68:607–619. doi: 10.1111/j.1365-313X.2011.04711.x

Beckett M, Loreto F, Velikova V, et al (2012) Photosynthetic limitations and volatile and non-volatile isoprenoids in the poikilochlorophyllous resurrection plant *Xerophyta humilis* during dehydration and rehydration. Plant, Cell Environ 35:2061–2074. doi: 10.1111/j.1365-3040.2012.02536.x

Benina M, Obata T, Mehterov N, et al (2013) Comparative metabolic profiling of *Haberlea rhodopensis*, *Thellungiella halophyla*, and *Arabidopsis thaliana* exposed to low temperature. Front Plant Sci 4:1–11. doi: 10.3389/fpls.2013.00499

Brüggemann W, Bergmann M, Nierbauer K, et al (2009) Photosynthesis studies on European evergreen and deciduous oaks grown under Central European climate conditions: II.Photoinhibitory and light-independent violaxanthin deepoxidation and downregulation of photosystem II in evergreen, winter-acclimated European *Quercus* taxa. 23:1091–1100. doi: 10.1007/s00468-009-0351-y

Buchner O, Stoll M, Karadar M, et al (2015) Application of heat stress in situ demonstrates a protective role of irradiation on photosynthetic performance in alpine plants. Plant, Cell Environ 38:812–826. doi: 10.1111/pce.12455

Buitink J, Leprince O (2008) Intracellular glasses and seed survival in the dry state. Comptes Rendus - Biol 331:788–795. doi: 10.1016/j.crvi.2008.08.002

Charuvi D, Nevo R, Shimoni E, et al (2015) Photoprotection conferred by changes in photosynthetic protein levels and organization during dehydration of a homoiochlorophyllous resurrection plant. Plant Physiol 167:1554–65. doi: 10.1104/pp.114.255794

Chaves MM, Flexas J, Pinheiro C (2009) Photosynthesis under drought and salt stress: Regulation mechanisms from whole plant to cell. Ann Bot 103:551–560. doi: 10.1093/aob/mcn125

Dall'Osto L, Cazzaniga S, Bressan M, et al (2017) Two mechanisms for dissipation of excess light in monomeric and trimeric light-harvesting complexes. Nat Plants 3:17033. doi: 10.1038/nplants.2017.33

Dall'Osto L, Cazzaniga S, Havaux M, Bassi R (2010) Enhanced photoprotection by protein-bound vs free xanthophyll pools: A comparative analysis of chlorophyll b and xanthophyll biosynthesis mutants. Mol Plant 3:576–593. doi: 10.1093/mp/ssp117

Degl'Innocenti E, Guidi L, Stevanovic B, Navari F (2008) CO2 fixation and chlorophyll a fluorescence in leaves of *Ramonda serbica* during a dehydration-

rehydration cycle. J Plant Physiol 165:723–733. doi: 10.1016/j.jplph.2007.06.009

Demmig-Adams B (1998) Survey of thermal energy dissipation and pigment composition in sun and shade leaves. Plant Cell Physiol 39:474–482. doi: 10.1093/oxfordjournals.pcp.a029394

Demmig-Adams B, Adams WW (2006) Photoprotection in an ecological context: the remarkable complexity of thermal energy dissipation. New Phytol 172:11–21.

Demmig-Adams B, Cohu CM, Muller O, Adams WW (2012) Modulation of photosynthetic energy conversion efficiency in nature: From seconds to seasons. Photosynth Res 113:75–88. doi: 10.1007/s11120-012-9761-6

Dubreuil M, Riba M, Mayol M (2008) Genetic structure and diversity in *Ramonda myconi* (Gesneriaceae): Effects of historical climate change on a preglacial relict species. Am J Bot 95:577–587. doi: 10.3732/ajb.2007320

Fernández-Marín B, Balaguer L, Esteban R, et al (2009) Dark induction of the photoprotective xanthophyll cycle in response to dehydration. J Plant Physiol 166:1734–1744. doi: 10.1016/j.jplph.2009.04.019

Fernández-Marín B, Becerril JM, García-Plazaola JI (2010) Unravelling the roles of desiccation-induced xanthophyll cycle activity in darkness: A case study in *Lobaria pulmonaria*. Planta 231:1335–1342. doi: 10.1007/s00425-010-1129-6

Fernández-Marín B, Hernández A, Garcia-Plazaola JI, et al (2017) Photoprotective strategies of mediterranean plants in relation to morphological traits and natural environmental pressure: a meta-analytical approach. Front Plant Sci 8:1051. doi: 10.3389/fpls.2017.01051

Fernández-Marín B, Holzinger A, García-plazaola JI (2016) Photosynthetic strategies of desiccation-tolerant organisms. In: Pessarakli M (ed) Handbook of Photosynthesis, Third Edition. CRC Press, Boca Raton, pp 663–681

Fernández-Marín B, Kranner I, Sebastián MS, et al (2013) Evidence for the absence of enzymatic reactions in the glassy state. A case study of xanthophyll cycle pigments in the desiccation-tolerant moss *Syntrichia ruralis*. J Exp Bot 64:3033–3043. doi: 10.1093/jxb/ert145

Fernández-Marín B, Míguez F, Becerril J, García-Plazaola J (2011a) Activation of violaxanthin cycle in darkness is a common response to different abiotic stresses: a case study in *Pelvetia canaliculata*. BMC Plant Biol 11:181. doi: 10.1186/1471-2229-11-181

Fernández-Marín B, Míguez F, Becerril JM, García-Plazaola JI (2011b) Dehydration-mediated activation of the xanthophyll cycle in darkness: Is it related to desiccation tolerance? Planta 234:579–588. doi: 10.1007/s00425-011-1420-1

Flores-Bavestrello A, Król M, Ivanov AG, et al (2016) Two Hymenophyllaceae species from contrasting natural environments exhibit a homoiochlorophyllous strategy in response to desiccation stress. J Plant Physiol 191:82–94. doi: 10.1016/j.jplph.2015.12.003

García-Plazaola JI, Becerril JM (2001) Seasonal changes in photosynthetic pigments and antioxidants in beech (*Fagus sylvatica*) in a Mediterranean climate: implications for tree decline diagnosis. Aust J Plant Physiol Aust J Plant Physiol 28:225–232. doi: 10.1071/PP00119

García-Plazaola JI, Esteban R, Fernández-Marín B, et al (2012) Thermal energy dissipation and xanthophyll cycles beyond the Arabidopsis model. Photosynth Res 113:89–103. doi: 10.1007/s11120-012-9760-7

Gashi B, Babani F, Kongjika E (2013) Chlorophyll fluorescence imaging of photosynthetic activity and pigment contents of the resurrection plants Ramonda serbica and Ramonda nathaliae during dehydration and rehydration. Physiol Mol Biol Plants 19:333–341. doi: 10.1007/s12298-013-0175-5

Georgieva K, Szigeti Z, Sarvari E, et al (2007) Photosynthetic activity of homoiochlorophyllous desiccation tolerant plant *Haberlea rhodopensis* during dehydration and rehydration. Planta 225:955–964. doi: 10.1007/s00425-006-0396-8

Gruszecki WI, Strzalka K (2005) Carotenoids as modulators of lipid membrane physical properties. Biochim Biophys Acta - Mol Basis Dis 1740:108–115. doi: 10.1016/j.bbadis.2004.11.015

Hacker J, Neuner G (2007) Ice propagation in plants visualized at the tissue level by infrared differential thermal analysis (IDTA). Tree Physiol 27:1661–70.

Hacker J, Spindelböck JP, Neuner G (2008) Mesophyll freezing and effects of freeze dehydration visualized by simultaneous measurement of IDTA and differential imaging chlorophyll fluorescence. Plant, Cell Environ 31:1725–1733. doi: 10.1111/j.1365-3040.2008.01881.x

Havaux M, Dall'Osto L, Cuiné S, et al (2004) The effect of zeaxanthin as the only xanthophyll on the structure and function of the photosynthetic apparatus in *Arabidopsis thaliana*. J Biol Chem 279:13878–13888. doi: 10.1074/jbc.M311154200

Hirsh AG (1987) Vitrification in plants as a natural form of cryoprotection. Cryobiology 24:214–28.

Holzwarth AR, Miloslavina Y, Nilkens M, Jahns P (2009) Identification of two quenching sites active in the regulation of photosynthetic light-harvesting studied by time-resolved fluorescence. Chem Phys Lett 483:262–267. doi: 10.1016/j.cplett.2009.10.085

Ilioaia C, Du CDP, Johnson MP, Ruban A V (2013) Antenna Induced by Xanthophyll Cycle Activity. J Phys Chem B 117:5841–5847.

Jahns P, Holzwarth AR (2012) The role of the xanthophyll cycle and of lutein in photoprotection of photosystem II. Biochim Biophys Acta - Bioenerg 1817:182–193. doi: 10.1016/j.bbabio.2011.04.012

Johnson MP, Goral TK, Duffy CDP, et al (2011) Photoprotective energy dissipation involves the reorganization of photosystem II light-harvesting complexes in the grana membranes of spinach chloroplasts. Plant Cell 23:1468–1479. doi: 10.1105/tpc.110.081646

Kappen L (1966) Der Einfluß des Wassergehaltes auf die Widerstandsfähigkeit von Pflanzen gegenüber hohen und tiefen Temperaturen, untersucht an Blättern einiger Farne und von *Ramonda myconi*. Flora 156:427–445. doi: 10.1016/S0367-1836(17)30278-1

Kosugi M, Arita M, Shizuma R, et al (2009) Responses to desiccation stress in lichens are different from those in their photobionts. Plant Cell Physiol 50:879–888. doi:

10.1093/pcp/pcp043

Kranner I, Beckett RP, Wornik S, et al (2002) Revival of a resurrection plant correlates with its antioxidant status. Plant J 31:13–24. doi: 10.1046/j.1365-313X.2002.01329.x

Kromdijk J, Glowacka K, Leonelli L, et al (2016) Improving photosynthesis and crop productivity by accelerating recovery from photoprotection.

Laza J, Julian C, Rodriguez M, Leon L (1999) Thermal scanning rheometer analysis of curing kinetic of an epoxy resin: 2. An amine as curing agent. Polymer (Guildf) 40:35–45. doi: 10.1016/S0032-3861(98)00217-1

Leuenberger M, Morris JM, Chan AM, et al (2017) Dissecting and modeling zeaxanthin- and lutein-dependent nonphotochemical quenching in *Arabidopsis thaliana*. Proc Natl Acad Sci U S A 114:E7009–E7017. doi: 10.1073/pnas.1704502114

Lundmark T, Bergh J, Strand M, Koppel A (1998) Seasonal variation of maximum photochemical efficiency in boreal Norway spruce stands. Trees 13:63. doi: 10.1007/s004680050187

Míguez F, Fernández-Marín B, Becerril JM, García-Plazaola JI (2017) Diversity of winter photoinhibitory responses: A case study in co-occurring lichens, mosses, herbs and woody plants from subalpine environments. Physiol Plant 160:282–296. doi: 10.1111/ppl.12551

Míguez F, Fernández-Marín B, Becerril JM, García-Plazaola JI (2015) Activation of photoprotective winter photoinhibition in plants from different environments: A literature compilation and meta-analysis. Physiol Plant 155:414–423. doi: 10.1111/ppl.12329

Müller J, Sprenger N, Bortlik K, et al (1997) Desiccation increases sucrose levels in *Ramonda* and *Haberlea*, two genera of resurrection plants in the Gesneriaceae. Physiol Plant 100:153–158. doi: 10.1111/j.1399-3054.1997.tb03466.x

Müller P, Li X-P, Niyogi KK (2001) Non-photochemical quenching. A response to excess light energy.

Nabe H, Funabiki R, Kashino Y, et al (2007) Responses to desiccation stress in bryophytes and an important role of dithiothreitol-insensitive non-photochemical quenching against photoinhibition in dehydrated states. Plant Cell Physiol 48:1548–1557. doi: 10.1093/pcp/pcm124

Neuner G (2014) Frost resistance in alpine woody plants. Front Plant Sci 5:654. doi: 10.3389/fpls.2014.00654

Neuner G, Erler A, Ladinig U, et al (2013) Frost resistance of reproductive tissues during various stages of development in high mountain plants. Physiol Plant 147:88–100. doi: 10.1111/j.1399-3054.2012.01616.x

Neuner G, Pramsohler M (2006) Freezing and high temperature thresholds of photosystem 2 compared to ice nucleation, frost and heat damage in evergreen subalpine plants. Physiol Plant 126:196–204. doi: 10.1111/j.1399-3054.2006.00605.x

Öquist G, Huner NPA (2003) Photosynthesis of overwintering evergreen plants. Annu Rev Plant Biol 54:329–355. doi: 10.1146/annurev.arplant.54.072402.115741

Ottander C, Oquist G (1991) Recovery of photosynthesis in winter-stressed Scots pine. Plant, Cell Environ 14:345–349. doi: 10.1111/j.1365-3040.1991.tb01511.x

Pearce R (2001) Plant Freezing and Damage. Ann Bot 87:417–424. doi: 10.1006/anbo.2000.1352

Picó FX, Riba M (2002) Regional-scale demography of *Ramonda myconi*: Remnant population dynamics in a preglacial relict species. Plant Ecol 161:1–13. doi: 10.1023/A:1020310609348

Porembski S, Barthlott W (2000) Granitic and gneissuc outcrops (inselbergs) as centers of diversity for desiccation tolerant vascular plants. Plant Ecol 151:19–28.

Rakic T, Gajic G, Lazarevic M, Stevanovic B (2015) Effects of different light intensities, CO2 concentrations, temperatures and drought stress on photosynthetic activity in two paleoendemic resurrection plant species *Ramonda serbica* and *R. nathaliae*. Environ Exp Bot 109:63–72. doi: 10.1016/j.envexpbot.2014.08.003

Rakić T, Lazarević M, Jovanović ŽS, et al (2014) Resurrection plants of the genus *Ramonda*: prospective survival strategies – unlock further capacity of adaptation, or embark on the path of evolution? Front Plant Sci 4:550. doi: 10.3389/fpls.2013.00550

Rapparini F, Neri L, Mihailova G, et al (2015) Growth irradiance affects the photoprotective mechanisms of the resurrection angiosperm *Haberlea rhodopensis* Friv. in response to desiccation and rehydration at morphological, physiological and biochemical levels. Environ Exp Bot 113:67–79. doi: 10.1016/j.envexpbot.2015.01.007

Riba M, Picó FX, Mayol M (2002) Effects of regional climate and small-scale habitat quality on per- formance in the relict species *Ramonda myconi*. J Veg Sci 13:259–268.

Ruban A V, Berera R, Ilioaia C, et al (2007) Identification of a mechanism of photoprotective energy dissipation in higher plants. Nature 450:575–578. doi: 10.1038/nature06262

Saga G, Giorgetti A, Fufezan C, et al (2010) Mutation analysis of violaxanthin de-epoxidase identifies substrate-binding sites and residues involved in catalysis. J Biol Chem 285:23763–23770. doi: 10.1074/jbc.M110.115097

Schwab KB, Schreiber U, Heber U (1989) Response of photosynthesis and respiration of resurrection plants to desiccation and rehydration. Planta 177:217–227. doi: 10.1007/BF00392810

Siljak-Yakovlev S, Stevanovic V, Tomasevic M, et al (2008) Genome size variation and polyploidy in the resurrection plant genus *Ramonda*: Cytogeography of living fossils. Environ Exp Bot 62:101–112. doi: 10.1016/j.envexpbot.2007.07.017

Strimbeck GR, Schaberg PG (2009) Going to extremes: low temperature tolerance and acclimation in temperate and boreal conifers. In: Gusta L, Wisniewski M, Tanino K (eds) Plant Cold Hardiness. CABI, pp 226–239

Strimbeck GR, Schaberg PG, Fossdal CG, et al (2015) Extreme low temperature tolerance in woody plants. Front Plant Sci 6:1–15. doi: 10.3389/fpls.2015.00884

Tian L, Magallanes-Lundback M, Musetti V, DellaPenna D (2003) Functional analysis of β- and ε-ring carotenoid hydroxylases in Arabidopsis. Plant Cell Online

15:1320–1332.

Tóth S, Kiss C, Scott P, et al (2006) *Agrobacterium*-mediated genetic transformation of the desiccation tolerant resurrection plant *Ramonda myconi* (L.) Rchb. Plant Cell Rep 25:442–449. doi: 10.1007/s00299-005-0083-4

Tóth S, Scott P, Sorvari S, Toldi O (2004) Effective and reproducible protocols for in vitro culturing and plant regeneration of the physiological model plant Ramonda myconi (L.) Rchb. Plant Sci 166:1027–1034. doi: 10.1016/j.plantsci.2003.12.020

Verhoeven A (2014) Sustained energy dissipation in winter evergreens. New Phytol 201:57–65.

Verhoeven A, García-Plazaola JI, Fernández-Marín B (2017) Shared mechanisms of photoprotection in photosynthetic organisms tolerant to desiccation or to low temperature. Environ Exp Bot. doi: 10.1016/j.envexpbot.2017.09.012

Verhoeven AS (2013) Recovery kinetics of photochemical efficiency in winter stressed conifers: the effects of growth light environment, extent of the season and species. Physiol Plant 147:147–158. doi: 10.1111/j.1399-3054.2012.01644.x

Verhoeven AS, Adams WW, Demmig-Adams B (1998) Two forms of sustained xanthophyll cycle-dependent energy dissipation in overwintering *Euonymus kiautschovicus*. Plant, Cell Environ 21:893–903. doi: 10.1046/j.1365-3040.1998.00338.x

Verhoeven AS, Adams WW, Demmig-Adams B (1996) Close relationship between the state of the xanthophyll cycle pigments and photosystem II efficiency during recovery from winter stress. Physiol Plant 96:567–576. doi: 10.1111/j.1399-3054.1996.tb00228.x

Wisniewski M, Gusta L, Neuner G (2014) Adaptive mechanisms of freeze avoidance in plants: A brief update. Environ Exp Bot 99:133–140. doi: 10.1016/j.envexpbot.2013.11.011

Zhang Y, Rempel C, Liu Q (2014) Thermoplastic starch processing and characteristics-A review. Crit Rev Food Sci Nutr 54:1353–1370. doi: 10.1080/10408398.2011.636156

Figures

Fig. 1 *Ramonda myconi* is a resurrection plant native to subalpine temperate environment and endemic to the Pyrinees. Its perennial leaves are able to survive both desiccation and freezing along the year. (A) *R. myconi* plant flowering in spring. (B) Frost of a *R. myconi* plant during Winter. (C) Desiccated plant at the end of summer in its natural population. (D) The same plant, after natural rehydration, two months later than in (C).

Fig. 2 Desiccation-rehydration cycle of *R. myconi* leaf-discs. Desiccation was performed under a RH of 50% and the whole cycle was conducted in darkness. Hydration is indicated in black and desiccation in white symbols and bars. (A) Maximal photochemical efficiency of PSII (F_v/F_m) ($n \geq 5$). (B) Changes in relative water content ($n \geq 5$). (C) Xanthophyll cycle de-epoxidation index (n=5). (D) Size of the total pigment pool of the xanthophyll cycle (n=5). (E) Relative amount of zeaxanthin to total chlorophyll (n=5). Data are means ± SE. When significant, differences in pigment contents among timepoints are depicted by lower case letters above the bars ($P<0.05$).

Fig. 3 Dynamic mechanical thermal analysis (DMTA) scans of *R. myconi* leaves desiccated at 50% RH (A, B), or hydrated (C, D). Shaded areas highlight the α-relaxation, which is identified as a peak or step in the Tan δ (upper panels: A, C), and as a deep decrease in the storage modulus (G') (lower panels: B, D). The α-relaxation corresponds to the transition from the glassy state (at lower temperatures), where molecular mobility is extremely limited, towards the gel state (at higher temperatures), where molecular mobility is much higher and enzymatic reactions progressively more likely to occur. Water content was 0.08 and 3.1 g H_2O g^{-1} DW in desiccated and in hydrated leaves, respectively.

Fig. 4 Dependence of the F_v/F_m on the actual air temperature. Values were recorded before sunrise during twelve winter days (in February and December 2016) in 1 to 2 leaves from 10 to 15 plants each time (specific number of leaves is detailed in italics underneath each box). Ice crystal symbol below the date denotes that all (whole symbol) or some (half symbol) of the sampled leaves were frozen during the measurement. Boxes cover 50% of the data; central lines represent the medians and whiskers represent the minimum and maximum values among non-atypical data. Open circles and asterisk represent outliers and extreme outliers, respectively. Significant differences are highlighted with lower case letters above each box ($P<0.05$).

Fig. 5 Recovery of winter-photoinhibited *R. myconi* leaves upon re-warming in the dark. (A) Maximal photochemical efficiency of PSII (F_v/F_m). (B) Xanthophyll cycle de-epoxidation index. (C) Relative amount of zeaxanthin to total chlorophyll. Leaves were collected frozen outdoor. Keep at +4 ˚C for the first hour and then at +20 ˚C during the rest of the recovery time. All this time, leaves were incubated in darkness, with liquid water in the petiole and at high RH. Data are means ± SE (n=3 biological replicates). When significant, differences among timepoints are depicted by lower case letters above the bars ($P<0.05$).

Fig. 6 Example of a *R. myconi* leaf subjected to a controlled freezing treatment from +4 to –7 ˚C at a cooling rate of 2 ˚K h^{-1}. Freezing of leaves was monitored with a digital infrared camera (A-E). A second set of leaves was measured by Differential Scanning Calorimetry (DSC) to estimate the ice nucleation temperature (F). (A) Original infrared image during the initial phase of freezing. (B, C) Images of the Infrared differential thermal analysis (IDTA) showing the first phase of freezing in which the ice spread through the xylem. Images were recorded 44 s and 57 s after initial ice nucleation in the petiole. (D, E) IDTA images showing the second phase of freezing in the mesophyll that took place approximately 6 min after the beginning of ice nucleation in the petiole. (F) DSC scan of winter *R. myconi* leaves recorded at 0.035 ˚C min^{-1} cooling rate. Exothermic peak reveals the ice nucleation event at around –2 ˚C.

Fig. 7 Changes in chlorophyll fluorescence and xanthophyll cycle pigments during controlled freezing of *R. myconi* leaves in darkness. (A) Basal fluorescence of Chl (F_0), expressed as % of the initial value measured at +4 ˚C, of three biological replicates monitored during cooling to –7 ˚C (cooling rate of 2 ˚K h^{-1}). Note: although F_0 was monitored in four leaves, the fluorometer probe moved during the measurement of one of them and F_0 is then only shown for three replicates. (B) F_v/F_m of the same four leaves (Feb 2016) plus further four leaves (Dec 2016) measured before (+4 ˚C) and at the end of the cooling treatment (–7 ˚C). Boxes cover 50% of the data; central lines represent the medians and whiskers represent the minimum and maximum values among non-atypical data (n=8). (C) Xanthophyll cycle de-epoxidation index of a separate set of leaves (Mar 2017) before (+4 ˚C) and after incubation in darkness at –7 ˚C for 16 h, representing a winter night. Data are average ± SE (n=6). (D) Relative amount of zeaxanthin to total chlorophyll of the same leaves. When significant, differences among timepoints are depicted by lower case letters above the bars (paired t-test, $P<0.05$).

FIGURES

Fig. 1

Fig.2

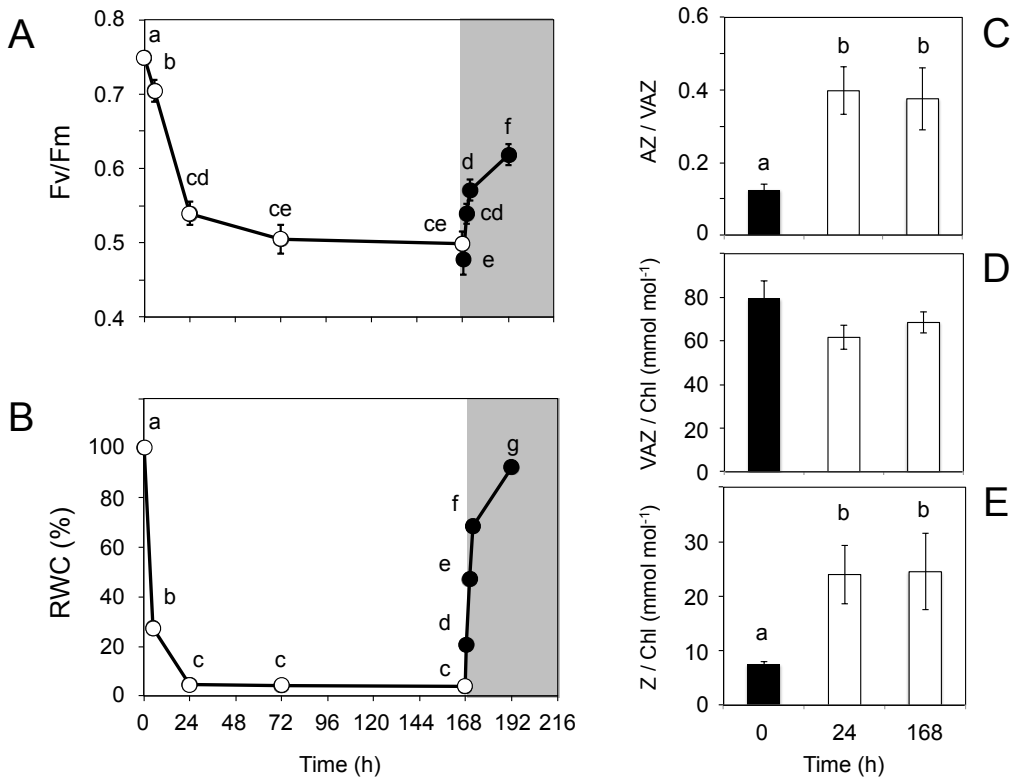
A
Fv/Fm
0.8
0.7
0.6
0.5
0.4
a
b
cd
ce
ce
d
f
cd
e
B
RWC (%)
100
80
60
40
20
0
a
b
c
c
c
d
e
f
g
0 24 48 72 96 120 144 168 192 216
Time (h)
C
AZ / VAZ
0.6
0.4
0.2
0
a
b
b
D
VAZ / Chl (mmol mol-1)
80
60
40
20
0
E
Z / Chl (mmol mol-1)
30
20
10
0
a
b
b
0 24 168
Time (h)

Fig.3

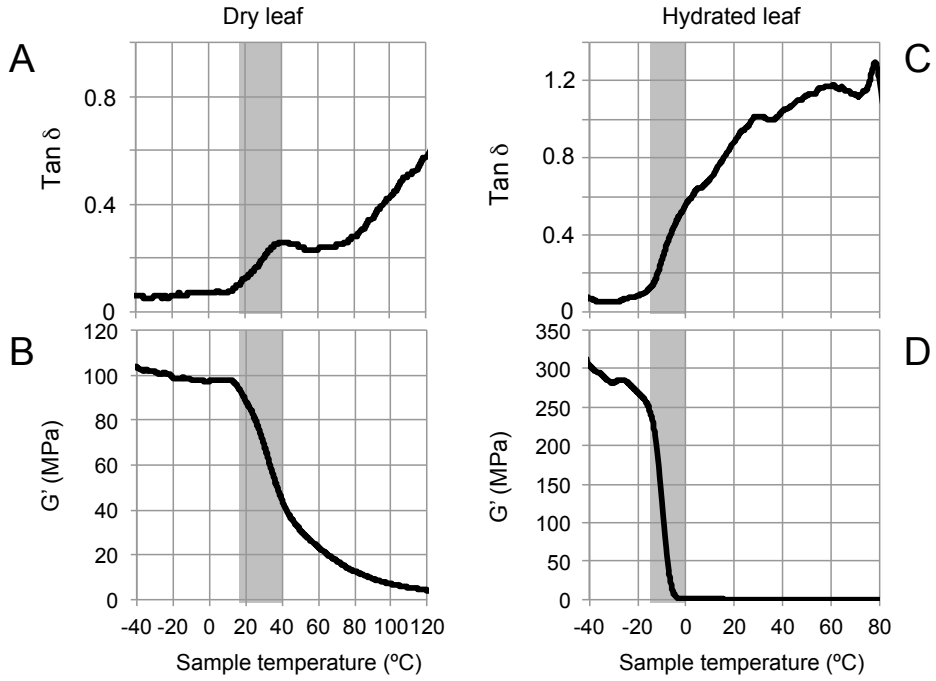
Dry leaf
Hydrated leaf
A
B
C
D
Tan δ
G' (MPa)
Sample temperature (ºC)
0
0.4
0.8
1.2
20
40
60
80
100
120
50
150
200
250
300
350
-40
-20

Fig. 4

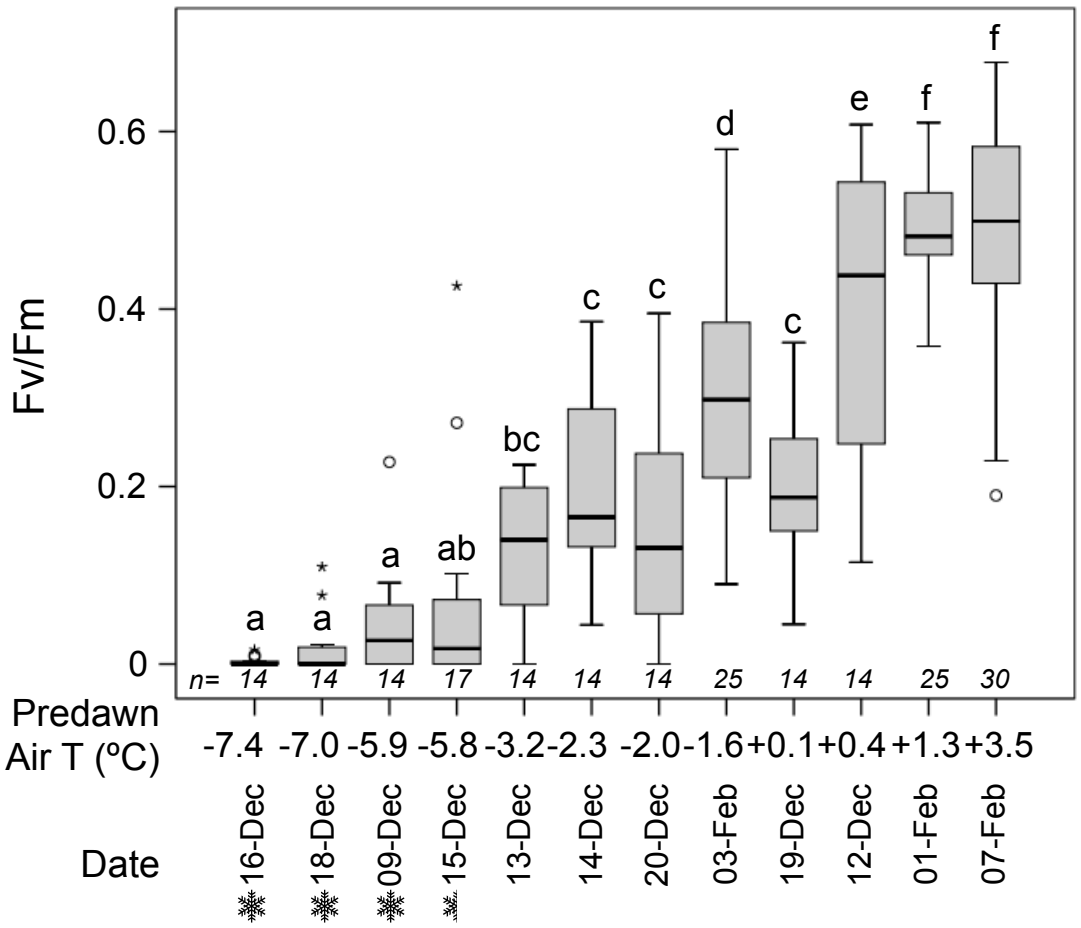
Fv/Fm
0.6
0.4
0.2
0
a
a
a
ab
bc
c
c
d
c
e
f
f
n= 14 14 14 17 14 14 14 25 14 14 25 30
Predawn Air T (ºC)
-7.4 -7.0 -5.9 -5.8 -3.2 -2.3 -2.0 -1.6 +0.1 +0.4 +1.3 +3.5
Date
16-Dec
18-Dec
09-Dec
15-Dec
13-Dec
14-Dec
20-Dec
03-Feb
19-Dec
12-Dec
01-Feb
07-Feb

Fig. 5

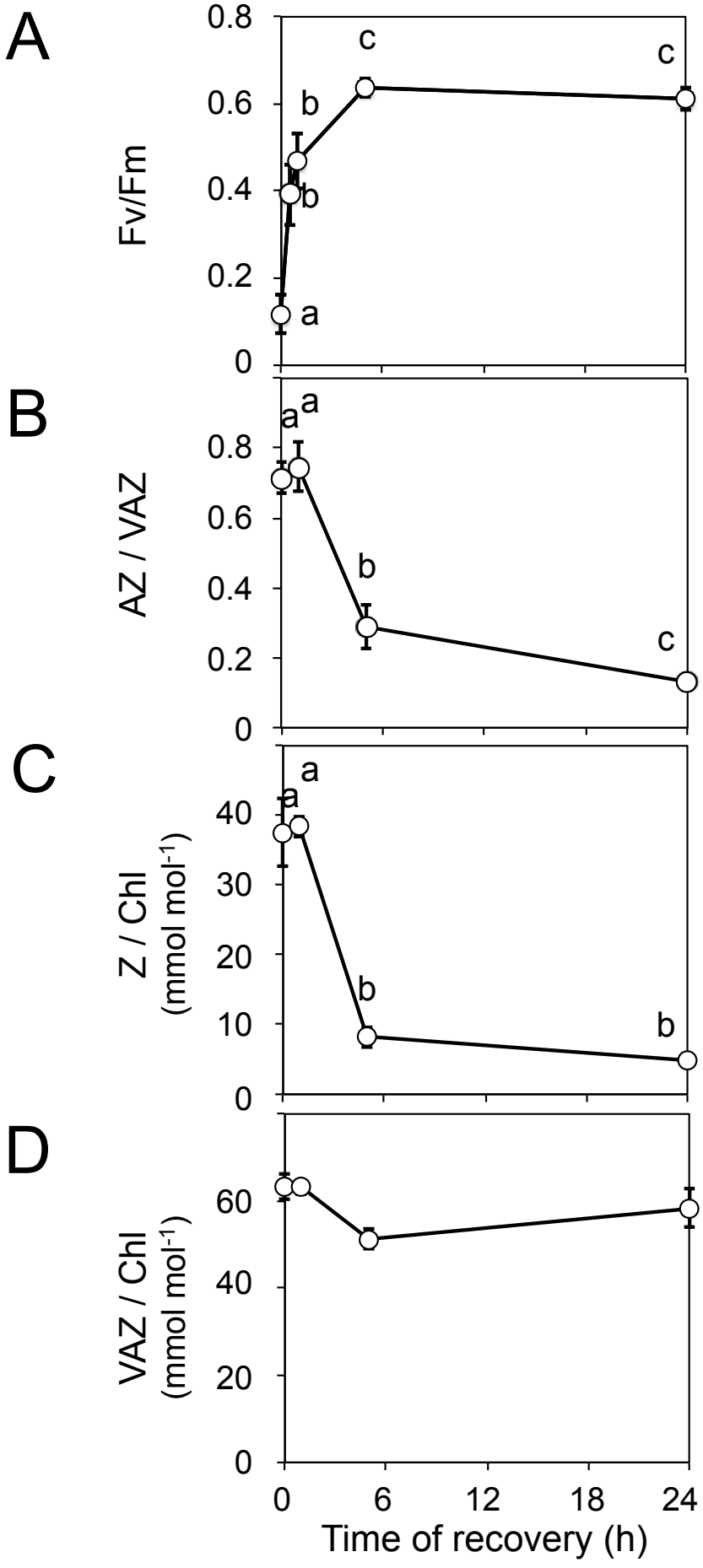
A
B
C
D
Fv/Fm
AZ / VAZ
Z / Chl
(mmol mol-1)
VAZ / Chl
(mmol mol-1)
Time of recovery (h)
0
6
12
18
24
0.2
0.4
0.6
0.8
10
20
30
40
60
a
b
c

Fig. 6

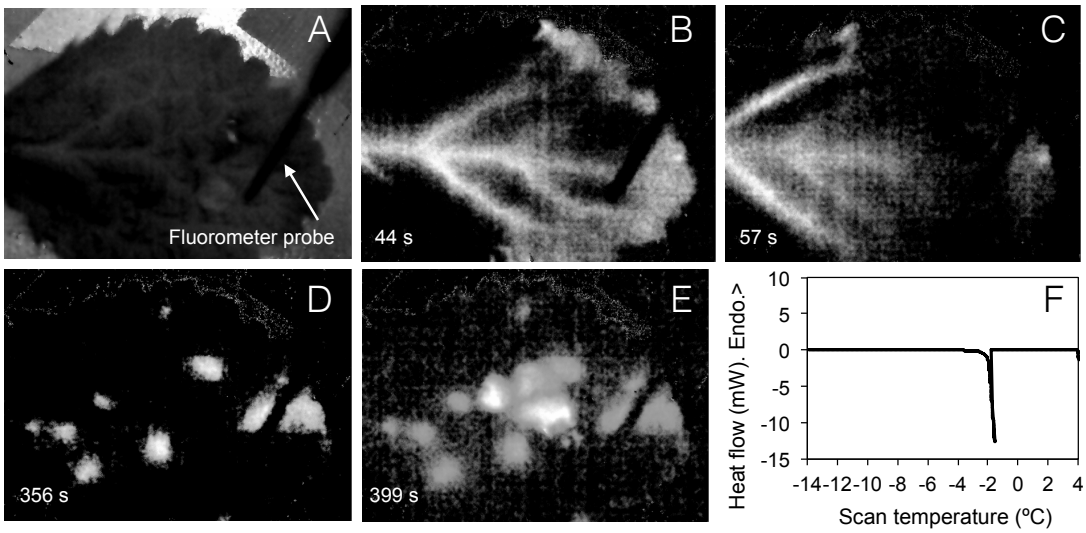
A
Fluorometer probe
B
44 s
C
57 s
D
356 s
E
399 s
F
Heat flow (mW), Endo.>
10
5
0
-5
-10
-15
-14 -12 -10 -8 -6 -4 -2 0 2 4
Scan temperature (ºC)

Fig. 7

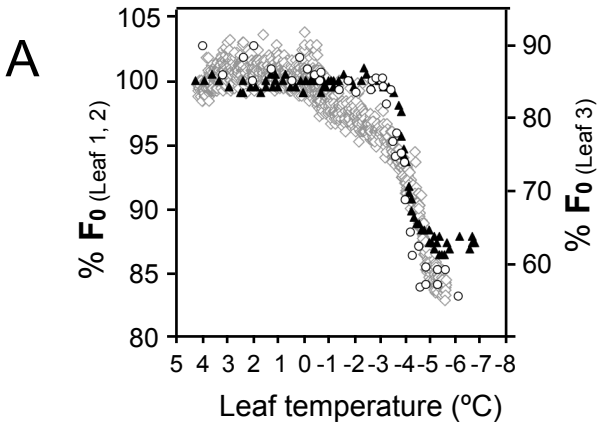
A
105
100
95
90
85
80
90
80
70
60
% F0 (Leaf 1, 2)
% F0 (Leaf 3)
5 4 3 2 1 0 -1 -2 -3 -4 -5 -6 -7 -8
Leaf temperature (ºC)

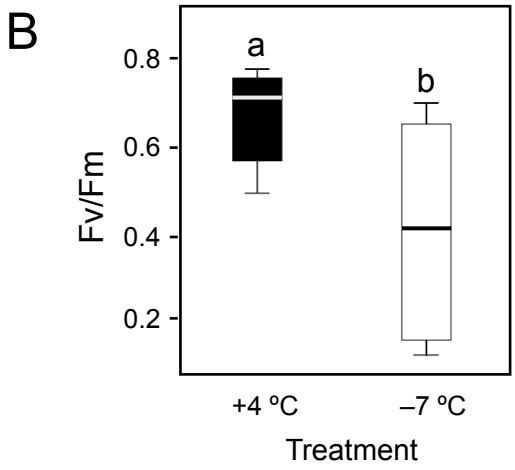
B
0.8
0.6
0.4
0.2
Fv/Fm
a
b
+4 ºC
–7 ºC
Treatment

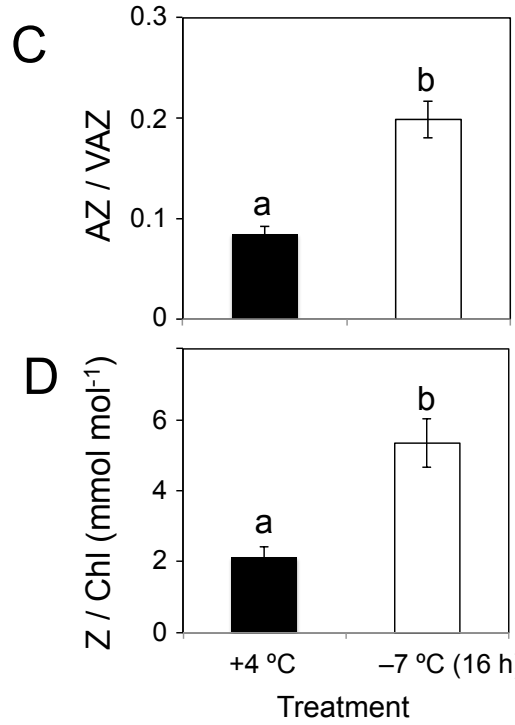
C
0.3
0.2
0.1
0
AZ / VAZ
a
b
D
6
4
2
0
Z / Chl (mmol mol-1)
a
b
+4 ºC
–7 ºC (16 h)
Treatment